Isolation of a Ribonucleoprotein Complex Involved in mRNA Localization in *Drosophila* Oocytes

James E. Wilhelm,[‡] Jennifer Mansfield,[§] Nora Hom-Booher,* Shengxian Wang,[§] Christoph W. Turck,* Tulle Hazelrigg,[§] and Ronald D. Vale*[‡]

[‡]Department of Cellular and Molecular Pharmacology and the *Howard Hughes Medical Institute, University of California, San Francisco, San Francisco, California 94143; and [§]Department of Biological Sciences, Columbia University, New York, New York 10027

Abstract. Localization of *bicoid* (*bcd*) mRNA to the anterior and *oskar* (*osk*) mRNA to the posterior of the *Drosophila* oocyte is critical for embryonic patterning. Previous genetic studies implicated *exuperantia* (*exu*) in *bcd* mRNA localization, but its role in this process is not understood. We have biochemically isolated Exu and show that it is part of a large RNase-sensitive complex that contains at least seven other proteins. One of these proteins was identified as the cold shock domain RNA-binding protein Ypsilon Schachtel (Yps), which we show binds directly to Exu and colocalizes with Exu in both the oocyte and nurse cells of the *Drosophila* egg chamber. Surprisingly, the Exu–Yps complex contains *osk* mRNA. This biochemical result led us to reexamine the role of Exu in the localization of *osk* mRNA. We discovered that *exu*-null mutants are defective in *osk* mRNA localization in both nurse cells and the oocyte. Furthermore, both Exu/Yps particles and *osk* mRNA follow a similar temporal pattern of localization in which they transiently accumulate at the oocyte anterior and subsequently localize to the posterior pole. We propose that Exu is a core component of a large protein complex involved in localizing mRNAs both within nurse cells and the developing oocyte.

Key words: oogenesis • nurse cells • cold shock domain • *oskar* mRNA • *exuperantia*

Introduction

Localization of mRNAs is used by many polarized cells as a means of restricting the distribution of a protein to a particular cytoplasmic domain (Bashirullah et al., 1998; Hazelrigg, 1998; St Johnston, 1995). Whereas the types of localized transcripts vary, mRNA localization in all systems shares several common features (Wilhelm and Vale, 1993; Macdonald and Smibert, 1996; Bassel and Singer, 1997; Gavis, 1997; Oleynikov and Singer, 1998). First, the cis-acting mRNA localization elements generally reside within the 3′ untranslated region (UTR)[1] (Kislauskis and Singer, 1992; Bashirullah et al., 1998). Second, the transport of localized messages from the nucleus to their final destinations occurs along either actin filaments or microtubule tracks. Third, transcripts are anchored at their sites of localization through attachments to cytoskeletal elements and then activated for translation. Although these phenomena have been well-documented, their molecular bases remain poorly understood.

One of the most extensively characterized systems for studying mRNA localization is the *Drosophila* oocyte. In the *Drosophila* egg chamber, an oocyte is linked to 15 nurse cells by a network of cytoplasmic bridges called ring canals (Spradling, 1993). The nurse cells synthesize various mRNAs that are required for early embryogenesis, such as the *bicoid* (*bcd*) and *oskar* (*osk*) transcripts, and transport them in a microtubule-dependent manner to discrete locations within the oocyte (Pokrywka and Stephenson, 1991, 1995). *bcd* mRNA is localized to the anterior of the oocyte (Berleth et al., 1988), and the resulting anterior–posterior gradient of the Bcd homeodomain protein initiates a series of concentration-dependent transcriptional programs that establish the anterior pattern of the embryo (St Johnston and Nusslein-Volhard, 1992). In contrast, *osk* mRNA is transported from the nurse cells to the anterior of the oocyte, but is ultimately localized to the posterior of the oocyte where it becomes stably anchored

Address correspondence to Ron Vale, Department of Cellular and Molecular Pharmacology, 513 Parnassus Ave., University of California, San Francisco, San Francisco, CA 94143. Tel.: (415) 476-6380. Fax: (415) 502-1391. E-mail: vale@phy.ucsf.edu

[1]*Abbreviations used in this paper: bcd, bicoid*; EST, expressed sequence tag; *exu*, *exuperantia*; GFP, green fluorescent protein; GST, glutathione *S*-transferase; HA, hemagglutinin; *nos*, *nanos*; *osk*, *oskar*; *pgk*, *phosphoglycerokinase*; RT; reverse transcribed; UTR, untranslated region; Yps, Ypsilon Schachtel.

(Ephrussi et al., 1991; Kim-Ha et al., 1991). The Osk protein synthesized at this location recruits a number of additional components that are required for the formation of the abdomen and germ cells (Ephrussi et al., 1991; Smith et al., 1992; Kobayashi et al., 1995; Breitwieser et al., 1996).

Genetic screens have identified several mutants that have patterning defects due to the mislocalization of *bcd* and/or *osk* mRNAs. Mutations in some genes, such as *swallow* and *staufen*, cause only partial disruption of *bcd* mRNA localization late in oogenesis (Berleth et al., 1988; Stephenson et al., 1988; St Johnston et al., 1989, 1991). However, in *exuperantia* (*exu*) mutants, defects in *bcd* mRNA localization occur early in oogenesis and result in *bcd* mRNA being uniformly distributed in the mature oocyte (Berleth et al., 1988; St Johnston et al., 1989). Time-lapse confocal microscopy has further shown that green fluorescent protein (GFP)-Exu forms particles that move in a microtubule-dependent manner and accumulate at the anterior and posterior of the oocyte (Theurkauf and Hazelrigg, 1998). Immunoelectron microscopy has also revealed that Exu is a component of large electron-dense structures called sponge bodies (Wilsch-Brauninger et al., 1997). However, all of these previous studies have not determined whether Exu is associated with transported mRNAs or whether its role is more indirect, such as in delivering material required for anchoring mRNA to the oocyte anterior.

Various studies have shown that localized messages are organized into particles (Ferrandon et al., 1994; Ainger et al., 1993; Bertrand et al., 1998), suggesting that a large protein complex may be involved in recognizing, transporting, and anchoring localized messages. However, identifying the proteins associated with localized mRNAs has been a difficult undertaking. Previous biochemical studies uncovered proteins that specifically recognize the RNA localization sequences in the 3′ UTR of mRNAs (MacDonald et al., 1995; Deshler et al., 1997; Ross et al., 1997; Havin et al., 1998; Hoek et al., 1998; Cote et al., 1999). However, their roles in mRNA transport have not been confirmed by genetic analyses. An alternative strategy is to isolate the native RNA complexes involved in mRNA transport and then identify the associated proteins. To achieve this goal, we thought that the Exu protein might provide a useful biochemical handle for the purification of an mRNA transport particle. In this study, we demonstrate that Exu exists in a large RNase-sensitive complex with at least seven other proteins, one of which is a cold shock domain RNA binding protein. Unexpectedly, *osk* mRNA is present in the Exu complex, and we have discovered that Exu is involved in posterior mRNA localization in addition to its previously described role in localizing mRNAs to the anterior. We propose that Exu is part of a core complex that localizes both *osk* and *bcd* mRNAs within nurse cells and the developing oocyte.

Materials and Methods

Drosophila Stocks

Oregon R (Ore) was the wild-type stock used for antibody staining and generation of wild-type *Drosophila* extracts. Females from NG5/NG5; Sco/SM1, which contains an X-linked insertion of a P[CasNGE] *gfp-exu* transgene (Wang and Hazelrigg, 1994), were used for double labeling of Ypsilon Schachtel (Yps) and Exu. For biochemical analysis, flies bearing a *gfp-exu-his*$_6$ transgene (16b-16) were used.

To construct the *gfp-exu-his*$_6$ transgene, the 5.5-kb SmaI-EcoRI *exu* genomic fragment was subcloned into pBlueScript II (SK) (Stratagene), to create pBS–*exu*5.5. pBS–*exu*5.5 was used as the template for in vitro mutagenesis to introduce BstEII and SphI restriction sites immediately upstream of *exu*'s translation start codon (using the Biorad Muta-Gene kit). Simultaneously, an 18-bp insertion encoding six histidine codons was introduced just upstream of *exu*'s stop codon. Correctly mutagenized plasmids were identified by restriction analysis for the presence of the BstEII and SphI sites, and DNA sequence analysis for the presence of the 18-bp his-encoding insertion. A 700-bp BstEII-SphI *gfp* fragment was excised from pEG1 (Wang and Hazelrigg, 1994), and subcloned into the BstEII and SphI sites of this mutagenized *exu* fragment. The resulting 6.2-kb *gfp-exu-his*$_6$ fragment was then excised by SmaI and EcoRI digestion and inserted into pCasPeR4 through its StuI and EcoRI cloning sites to create pWG16b. P-element transformation followed standard injection protocols (Spradling and Rubin, 1982), with transposase activity provided by the recipient strain (*y w; Sb 2-3/TM6*). A transformant line bearing an insertion on the X chromosome was established (*w, 16b-16*), and genetic crosses with an *exu*^{SCO2}/*CyO* strain determined that the *gfp-exu-his*$_6$ transgene rescued the female sterility associated with the *exu*^{SCO2} mutation.

Extract Preparation

Extracts were prepared by flash freezing 50–60 ml of flies in liquid N_2. The frozen flies were ground to a fine powder with a prechilled mortar and pestle, with regular additions of liquid N_2 to keep the sample frozen. The fly powder was degassed for 5–10 min on ice in a 50-ml Falcon tube and mixed either 1:1 or 1:2 with *Drosophila* extract buffer (DXB: 25 mM Hepes, pH 6.8, 50 mM KCl, 1 mM $MgCl_2$, 1 mM DTT, 250 mM sucrose) containing 10 μg/ml aprotinin, leupeptin, pepstatin, and 1 mM PMSF. The extracts were homogenized with 10 strokes of the B dounce in a 50-ml dounce homogenizer, followed by 10 strokes of the A dounce, and then centrifuged at 10,000 *g* for 15 min at 4°C in the Beckman TLX ultracentrifuge. The supernatant was collected and centrifuged a second time. The supernatant from the second spin was collected, aliquoted, frozen in liquid N_2, and stored at −80°C. Hand dissected extracts were prepared by dissecting 50 ovaries into 0.7 ml of modified *Drosophila* extract buffer (mDXB: 25 mM Hepes, pH 6.8, 50 mM KCl, 1 mM $MgCl_2$, 1 mM DTT, 125 mM sucrose) containing 10 μg/ml aprotinin, pepstatin, leupeptin, and 1 mM PMSF. The sample was then homogenized with 15 strokes in a 2-ml dounce homogenizer (Wheaton, Inc.) at 4°C. The extract was centrifuged at 10,000 *g* for 10 min at 4°C to collect the supernatant.

Sucrose Density Gradient Analysis of Exu Complex

Extract from hand dissected ovaries (250 μl) was loaded on a 5-ml 5–40% sucrose gradient made with DXB containing 10 μg/ml leupeptin, pepstatin, and aprotinin. For frozen *Drosophila* extracts, 150 μl of ~10 mg/ml extract was diluted 1:1 with sucrose-free DXB containing 10 μg/ml pepstatin, leupeptin, aprotinin, and 1 mM PMSF. The diluted extract was centrifuged at 10,000 *g* for 5 min in a microcentrifuge and the supernatant loaded on a 5-ml 5–40% sucrose gradient. The gradients were centrifuged at 237,000 *g* for 4 h in a Beckman SW-55 rotor. 300-μl fractions were collected from the gradient and precipitated with 1/10 volume TCA using 20 μg aprotinin as a carrier. The precipitate was resuspended in 30 μl sample buffer and 15 μl was loaded onto SDS-PAGE gel for immunoblot analysis. For RNase shift experiments, the extract (250 μl) was either treated with 2.5 μg of RNase A for 10 min at 4°C, followed by addition of 2,000 U of RQ1 RNasin (Promega), or treated for 10 min at 4°C with 2.5 μg of RNase A that had been preincubated with 2,000 U of RQ1 RNasin. These samples were loaded onto a 5-ml 10–40% sucrose gradient and centrifuged as above.

Two-Step Purification of GFP-Exu-His$_6$

5 ml of ~10 mg/ml *Drosophila* extract (made with 5 mM β-mercaptoethanol instead of 1 mM DTT) were incubated with 0.5 ml of Ni-NTA resin in the presence of 0.1% Triton X-100 for 1 h at 4°C. The resin was washed once in batch with 10 ml of DXB150 (DXB with 150 mM KCl) supplemented with 0.1% Triton X-100 (wash 1) followed by a 10-ml column wash (wash 2). The column was eluted with 250 mM imidazole in

DXB150, and 0.5-ml fractions collected. The peak fractions were pooled and immunoprecipitated as described.

Antibody Generation

The full-length coding region and the first 160 amino acids of Yps (Yps160) were each cloned into pGEX-2T and expressed as COOH-terminal fusions to glutathione *S*-transferase (GST) in *E. coli*. Soluble GST-Yps and GST-Yps160 were purified on a glutathione affinity column, eluted with glutathione, and injected into rabbits (antiserum production by BABCO). GST-Yps did not express as a full-length protein in *E. coli*, but rather yielded a protein product ~10 kD larger than GST-Yps160. Antisera to GST-Yps160 was affinity purified by preabsorption on an Affi-Gel column coupled with GST, followed by affinity purification with an Affi-Gel column coupled with GST-Yps160. This affinity purified antibody was used for all experiments except for those shown in Fig. 8, C and D, where the GST-Yps antisera was used. The antisera against GST-Yps gave identical results to the affinity purified anti-Yps160 antibody in immunofluorescence experiments.

GFP was expressed in *E. coli* and purified on a Q-Sepharose column followed by a phenyl Sepharose column. The purified GFP was injected into rabbits for antisera production (BABCO). Antisera to GFP was affinity purified with an Affi-Gel column coupled with GFP. This antibody recognizes GFP in both immunoblots and immunoprecipitations.

Antisera against a peptide (NRRGGRQSVKDARPSSC; amino acids 422–437) from Exu were generated (QCB, Inc.) and affinity purified with peptide coupled to Sulfolink gel (Pierce, Inc.). This affinity purified antibody recognizes Exu in both immunoblots and immunoprecipitations.

Immunoblots

For immunoblot analysis, samples were run on SDS–polyacrylamide gels and then transferred to nitrocellulose by semidry transfer. The membrane was blocked in TBS (20 mM Tris-Cl, pH 7.5, 200 mM NaCl), 0.1% Tween 20, 10% nonfat dry milk, and then incubated with either 1:2,000 dilution of anti-Exu rabbit antibody (gift of Paul MacDonald, University of Texas at Austin, Austin, TX) or 5 μg/ml of affinity purified anti-Yps rabbit antibody in TBS, 0.1% Tween 20, 5% BSA. Protein was detected by chemiluminescence using HRP-conjugated donkey anti–rabbit Ig (Amersham Pharmacia Biotech) diluted 1:2,500 in TBS containing 0.1% Tween 20 and 5% BSA.

Immunoprecipitations of Yps and GFP

125 μl of protein A agarose beads (GIBCO BRL) was washed six times with PBS (137 mM NaCl, 2.6 mM KCl, 10 mM $NaHPO_4$, 1.7 mM KH_2PO_4) + 0.1% Triton X-100 (PBST). 50 μg of antibody was added to the beads in a final volume of 300 μl and mixed for 30 min at room temperature. The beads were washed once with PBST followed by two washes with 0.2 M sodium borate, pH 9.0. Dimethyl pimelidate was then added to a final concentration of 20 mM and the sample mixed for 1 h at room temperature. The beads were washed three times with 0.2 M ethanolamine, pH 8.0, and mixed for 2 h at room temperature. The beads were preeluted with three 1-ml washes of 100 mM glycine, pH 2.5, followed by three washes with DXB.

Fresh 10 μg/ml leupeptin, pepstatin, and 1 mM PMSF were added to 1 ml of frozen *Drosophila* extract (~10 mg/ml) and centrifuged at 10,000 *g* for 5 min in a microcentrifuge. 850 μl of supernatant was immunoprecipitated with 50 μl of antibody-coated beads for 1 h at 4°C with gentle shaking. The beads were washed four times with DXB containing 10 μg/ml leupeptin, pepstatin, and 1 mM PMSF and then eluted with two 150-μl washes and one 200-μl wash of 100 mM glycine, pH 2.5. The elutions were neutralized with 200 μl of 0.5 M Hepes, pH 7.6, and any residual beads removed by centrifuging at 10,000 *g* for 5 min in a microcentrifuge. The supernatant was precipitated with 1/10 volume TCA in the presence of 20 μg aprotinin as a carrier. The sample was resuspended in sample buffer for further analysis. When RNase sensitivity of the immunoprecipitation was assayed, the incubation of extract with antibody-coated beads was performed in the presence of 300 μg of RNase A. Immunoprecipitations of the Exu complex from sucrose gradients were performed on fractions pooled from five 5–40% sucrose gradients loaded with frozen *Drosophila* extract using our standard conditions (see above).

Microsequence Analysis of p57/Yps

p57 was immunoprecipitated as described, separated by SDS-PAGE, and then stained with Coomassie blue. After removing the protein band, an in-gel digestion with Endoproteinase Lys-C (Roche Diagnostics) was carried out as described (Hellman et al., 1995). Gel-extracted peptides were then fractionated using a Vydac microbore C8 column (The Separations Group), and individual peptides subjected to Edman degradation with a protein sequencer, Model 492 (PerkinElmer Biosystems). BLAST searches with these peptides identified p57 as Yps. Six expressed sequence tags (ESTs) corresponding to *yps* (GM14045, LD01826, GM03816, LD18388, GM02535, LD01538) were obtained (Berkeley *Drosophila* Genome Project/Howard Hughes Medical Institute EST Project) and sequenced.

Immunoprecipitations for Reverse Transcribed–PCR

Immunoprecipitations were carried out as above, but the antibody was not cross-linked to the protein A agarose beads (GIBCO BRL). Beads were washed four times with DXB200 (DXB, with 200 mM KCl) containing 10 μg/ml leupeptin, pepstatin, and 1 mM PMSF. Beads were then resuspended in 200 μl buffer (100 mM Hepes, pH 6.8, 150 mM NaCl, 12.5 mM EDTA, 1% SDS) and heated to 65°C for 10 min. The beads were pelleted and the supernatant from two immunoprecipitations was phenol/chloroform-extracted followed by an ethanol precipitation using 20 μg glycogen as carrier. The pellet was resuspended in 50 mM Hepes, pH 6.8, 1 mM $MgCl_2$ and treated with 10 U RQ1 DNase I (Promega) for 30 min at 37°C. The sample was then phenol/chloroform-extracted, and ethanol-precipitated a second time. The RNA sample was reverse transcribed (RT) using the Superscript preamplification system (GIBCO BRL), and 2 μl of 10-, 100-, and 1,000-fold dilutions of the RT product were amplified in a 50-μl PCR reaction (20 mM Tris-HCl, pH 8.4, 50 mM KCl, 1.5 mM $MgCl_2$, 1 mM dNTPs, 2.5 U *Taq* polymerase, 15 pmol primer). Cycling conditions were 5 min at 95°C, followed by 40 cycles of 1 min at 95°C, 1 min at 55°C, and then 1 min at 72°C. Primers were tested by using the same RT-PCR conditions as above, except 5 μg of total RNA from extracts was used in the RT reaction and only 30 cycles of PCR were performed. The primers used were: bcd2761, 5′-gtcggatcctgggtcgaccaatgtcaatggcg-3′; bcd3738, 5′-gtcgaattcgctcttgtccagacccttcaaagg-3′; osk860, 5′-gtcggatccaatggaatcacgatatcgagcatca-3′; osk1630, 5′-gtcgaattcttacgctggcttgctggtagaaat-3′; nos1110, 5′-gtcggatccgatccttgaaaatctttgcgcaggt-3′; nos2221, 5′-gtcgaattctcgttgttattctcacaaaagacgca-3′; pgk1800, 5′-gtcggatccgccaagaagaataacgtgcagttgc-3′; and pgk2280, 5′-gtcgaattccgctggtcaatgcacgcacgc-3′. RT-PCR primers were designed for *osk*, *nanos* (*nos*), and *bcd* to span an intron to easily separate RT-PCR products from products that were amplified due to genomic contamination. Products for *osk*, *nos*, and *bcd* were subcloned and their identity confirmed by DNA sequencing.

Immunofluorescence

0–1-d-old females were collected and fed for 1–2 d with dried baker's yeast, in the presence of males. Ovaries were dissected into PBT and fixed in 600 μl of heptane and 100 μl of fixative (6% formaldehyde, 16.7 mM KPO_4 pH 6.8, 75 mM KCl, 25 mM NaCl, 3.3 mM $MgCl_2$) rocking at room temperature for 9 min. The ovaries were then washed several times in PBT, for a total of 15 min. Ovaries were permeabilized in PBT for 5 h, blocked in 0.5% BSA in PBT for 30 min, and incubated in a 1:500 dilution of the primary antibody in PBT overnight at 4°C. The secondary antibody (rhodamine-conjugated goat anti–rabbit Fab fragments; Jackson Immunochemical Research, Inc.) was simultaneously preabsorbed to fixed ovaries at a dilution of 1:500 in PBT overnight at 4°C. After removal of the primary antibody, the ovaries were washed in PBT (five times for 5 min) at room temperature, and incubated in the preabsorbed secondary antibody for 3 h at room temperature. The ovaries were then washed in PBT (five times for 5 min), and either mounted in 20 μl Fluoromount-G (Southern Biotechnology Associates, Inc.) or incubated overnight in 60% glycerol in PBT at 4°C, then mounted in 40 μl of 60% glycerol. Imaging was performed on a Biorad MRC600 laser confocal unit attached to a Zeiss Axioplan microscope.

Binding Assays for In Vitro Translated Exu and Yps

Site-directed mutagenesis and PCR were used to create unique restriction sites in order to attach NH_2-terminal epitope tags in-frame to *exu* and *yps* cDNAs. DNA encoding the 3× myc tag was obtained from T7myc-Gsp1wt vector (gift of Erin O'Shea, University of California, San Francisco, San Francisco, CA) and joined to the 5′ end of *yps*. DNA encoding the 3× hemagglutinin (HA) tag was obtained from the pGTEP vector (gift of Joachim Li, University of California, San Francisco) and joined to the 5′ end of *exu*.

Each of the two fusions was then subcloned into the NcoI and EcoRI sites of the pSPBPI transcription vector (gift of Vishu Lingappa, University of California, San Francisco); this vector was derived from pSP64 and includes a 5′ UTR and strong Kozak consensus region from *Xenopus* globin cDNA.

A coupled transcription–translation system (Promega) was used to in vitro translate tagged Exu and Yps. 600 ng of plasmid DNA was added to a 50-μl transcription–translation mix. The myc-Yps transcription–translation mix contained [^{35}S]methionine (Translabel; ICN), whereas the HA–Exu mix did not. After a 90-min incubation at 30°C, 0.5 μl of 400 nM 7-methylguanosine 5-monophosphate (CAP Analogue) and 5 μl of 10 mg/ml RNase A were added to each reaction. 5 μl of radiolabeled myc-Yps was either incubated alone or mixed with cold HA–Exu and coincubated for 30 min at room temperature. Afterwards, 490 μl of DXBT250 (DXB containing 250 mM KCl and 0.1% Triton X-100) was added to the coincubation mixes before the immunoprecipitations.

For immunoprecipitations, 0.5 μl of anti-HA (16S12 monoclonal; gift of Dave Morgan) was added to translations and set on a rotator at 4°C for 60 min. A 30-μl slurry containing 10 μl of protein A beads (Life Technologies, Inc.) was added to the translation–antibody mix and incubated for another 60 min at 4°C on a rotator. The beads were then pelleted in a low-speed microfuge for 2 min and the supernatant was removed. After washing with DXBT250 (three times in 1 ml), the beads were resuspended in SDS sample buffer and boiled for 5 min. 7.5 μl was loaded on 4–12% SDS-PAGE gel and processed for autoradiography.

osk In Situ Hybridization

Whole mount in situ hybridization to ovaries was performed as described previously (Tautz and Pfeifle, 1989) with several modifications. Ovaries from well-fed, 2–3-d-old females raised at 18°C (Oregon R or *exu*^{SC02}/Df[2]MK1) were dissected into PBT and fixed for 15 min in 8:1:1 (4% paraformaldehyde in PBT/Clorox bleach/dimethyl sulfoxide). The ovaries were washed twice for 5 min in PBT, and 5 min each in 3:1, 1:1, and 1:3 PBT/methanol, then twice for 5 min in methanol, and stored at −20°C. Before hybridization, the ovaries were rehydrated into PBT by 5-min washes in 3:1, 1;1, 1:3 methanol/PBT and twice for 5 min in PBT. After teasing apart the ovarioles slightly, the ovaries were treated for 15 min with 50 μg/ml proteinase K (Boehringer Mannheim) in PBT, washed twice quickly in PBT, and postfixed for 10 min in 4% paraformaldehyde in PBT. After five 5-min washes in PBT, the ovaries were equilibrated into hybridization buffer (HB: 5×SSC, 0.1% Tween 20, 50 μg/ml heparin, 0.1 mg/ml denatured salmon sperm DNA, 50% formamide) by 5-min incubations in 3:1, 1:1, and 1:3 PBT/HB, followed by a 1-h incubation at 45°C in HB. Hybridization was done in 10 μl of probe in HB (see below) overnight at 45°C. Excess probe was removed by three 20-min washes in HB, followed by 10-min washes in 3:1, 1:1, and 1:3 HB/PBT, all at 45°C. The ovaries were then washed five times for 5 min in PBT at room temperature, then incubated in an alkaline phosphatase–conjugated antidigoxygenin antibody (Boehringer Mannheim) at a dilution of 1:2,000 in PBT for 1 h. Before incubation, the antibody was preabsorbed to fixed ovaries for at least 1 h. The ovaries were washed five times for 5 min in PBT and twice for 5 min in alkaline phosphatase staining buffer (100 mM NaCl, 50 mM $MgCl_2$, 100 mM Tris, pH 9.5, 0.1% Tween 20). For antibody detection, 1 ml alkaline phosphatase staining buffer, 4.5 μl 4-nitro blue tetrazolium chloride, and 3.5 μl X-phosphate (Boehringer Mannheim) were added to the ovaries and incubated 3–10 min. We found that a short staining time was crucial in order to prevent saturation of the color reaction, which masked differences between the genotypes. The ovaries were then washed several times in PBT for a total of 45 min and equilibrated overnight at 4°C in 60% glycerol. Ovaries were mounted in 60% glycerol and visualized on a Nikon Eclipse E800 microscope with a Nikon Plan Fluor 20× objective, under Nomarski optics. Photographs were taken with a Nikon FX-35WA camera on Kodak Elite Chrome slide film, and scanned into Adobe Photoshop with a Polaroid SprintScan 35 slide scanner.

Probes were prepared by labeling a plasmid containing the *osk* cDNA, PNBosk7 (courtesy of R. Lehmann, Skirball Insitiute, New York University Medical Center, New York, NY) with dig-dUTP using DIG-Nick Translation Mix (Boehringer Mannheim). After ethanol precipitation, the probe was resuspended in 100 μl HB. Just before use, the probe was denatured by boiling for 5 min, and cooled on ice.

Results

Exu Exists in a Large RNase-sensitive Complex

To define the biochemical properties of Exu, we determined its size in *Drosophila* extracts using sucrose density gradients. In extracts made from either hand dissected ovaries (Fig. 1 A) or whole flies that were frozen in liquid N_2 (data not shown), Exu migrated in a very broad distribution with a significant fraction of Exu migrating larger than 20 S (Fig. 1 A). In contrast, in vitro–translated Exu sedimented at 4.5 S, the value expected of a monomeric 58-kD protein (data not shown). Therefore, the large size of Exu in *Drosophila* extracts must be due to its association with additional proteins and/or RNAs. To test whether the Exu complex contains RNA, the extract was treated with RNase A before sedimentation analysis. This treatment caused the complex to migrate as a 7-S species; this shift was not due to proteolysis, since a control reaction in which RNase A was premixed with RNase inhibitor did not affect Exu migration (Fig. 1 B). These results demonstrate that Exu is associated with a large RNA-containing complex.

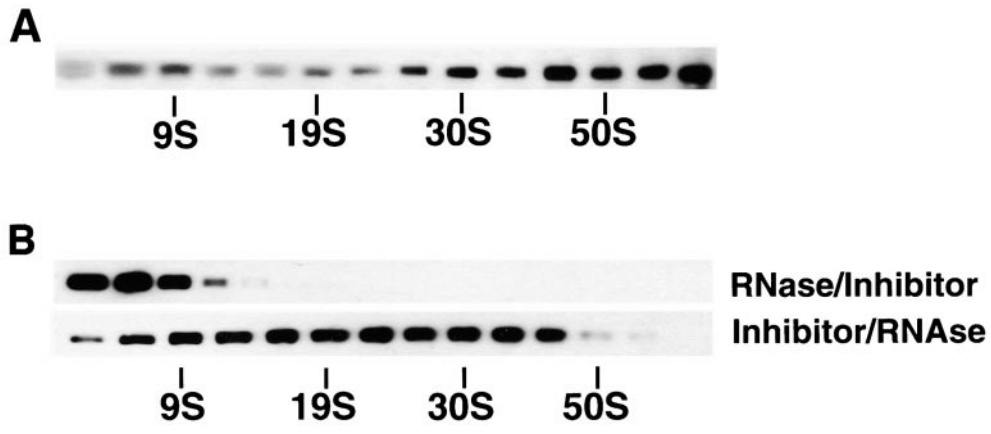

Figure 1. RNase-sensitive sedimentation of Exu in *Drosophila* extracts. (A) Sedimentation of Exu from an extract made from hand dissected ovaries through a 5–40% sucrose gradient (see Materials and Methods). This immunoblot shows a broad distribution of Exu signal with the majority sedimenting >20 S. (B) Sedimentation of Exu in extracts treated with RNase A (10 μg/ml, 10 min at 4°C) followed by addition of pancreatic RNase inhibitor (8,000 U/ml) (upper panel). As a control, RNase A was premixed with the inhibitor before addition to the extract (lower panel). When RNase A is added first, the Exu immunoblot signal shifts from a large broad distribution to a tight 7-S peak. Although there is some variability in the sedimentation profile of Exu from extract to extract, there is always a significant fraction of Exu sedimenting at 20 S or greater.

The RNA-binding Protein Yps Copurifies with Exu

To identify the protein components of the Exu complex, GFP-Exu was immunoprecipitated from whole fly extracts prepared from a GFP-Exu–expressing fly line using an anti-GFP antibody. The GFP tag does not impair Exu protein function, since the *gfp-exu* transgene fully complements a null allele of *exu* (*exu*^{SCO2}) (Wang and Hazelrigg, 1994). Fig. 2 shows that seven polypeptides of 57, 74, 76, 78, 82, 88, and 147 kD coimmunoprecipitated specifically with GFP-Exu, but not with control IgG-coated beads. A similar set of polypeptides coimmunoprecipitated with GFP-Exu from an extract made from hand dissected ovaries, indicating that this complex is present within the female germ line (data not shown). This same set of polypeptides also coimmunoprecipitated with Exu from wild-type fly extracts using an antibody directed against a COOH-terminal peptide of Exu (data not shown; see Materials and Methods). Of the coimmunoprecipitated proteins, the 57-, 74-, 76-, 78-, and 82-kD proteins were present in amounts comparable to that of GFP-Exu, whereas the 88- and 147-kD proteins were clearly substoichiometric. When the extract was extensively treated with RNase A, only the 57-kD protein remained associated with GFP-Exu (Fig. 2). Taken together with our gradient analysis (Fig. 1 B), these results suggest that Exu and p57 are components of a 7-S RNase-resistant core complex; the other polypeptides (p74, p76, p78, p82, p88, and p147) all require the presence of RNA in order to associate with Exu.

To confirm that the 57-kD polypeptide was a bona fide Exu-associated protein, we used a different purification strategy to isolate Exu complexes. Using flies that express Exu with an NH_2-terminal GFP tag and a COOH-terminal His_6 tag, extracts were subjected to a two-step purification consisting of binding to an Ni-NTA column, elution with imidazole, and then immunoprecipitation with the anti-GFP antibody (Fig. 3). The 57-kD protein consistently copurified stoichiometrically with GFP-Exu-His_6 through this two-step affinity purification, confirming that it is a true Exu-associated polypeptide. The other polypeptides in the 74–82 kD range were identified in some of our preparations, but their presence and amount was highly variable, possibly due to RNA degradation during the procedure or instability of the complex during imidazole elution from the column.

To identify the 57-kD Exu-associated protein, we mi-

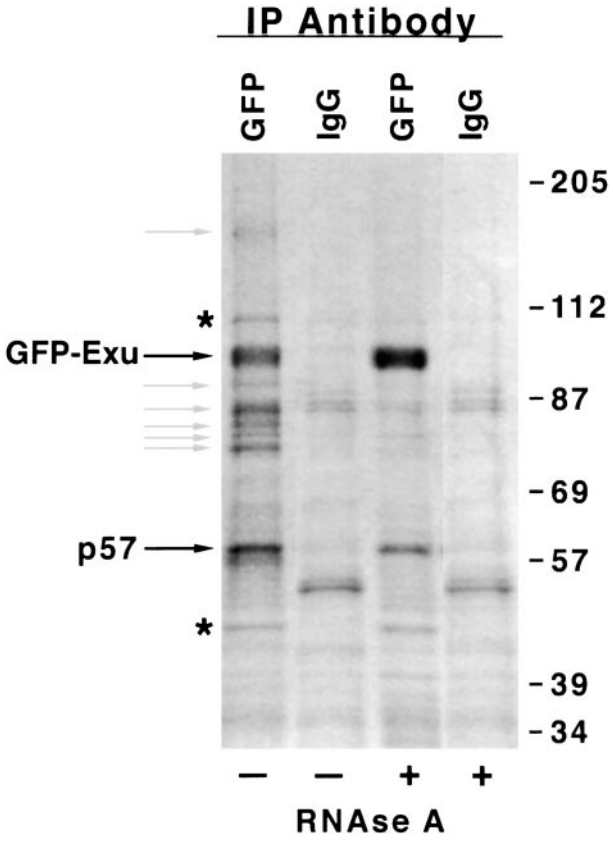

Figure 2. Immunoprecipitation of Exu-associated proteins. Immunoprecipitations of GFP-Exu extracts were performed with either anti-GFP antibodies or rabbit IgG. GFP-Exu and seven additional polypeptides (arrows) coimmunoprecipitate with anti-GFP antibodies, but not with the rabbit IgG control. RNase A treatment of the extracts during the immunoprecipitation shows that six of the associated polypeptides (grey arrows) require the presence of RNA to coimmunoprecipitate with GFP-Exu, whereas p57 (dark arrow) does not. Two additional proteins, p110 and p45, are also present in some immunoprecipitations (asterisks). p110 only associates with Exu nonspecifically in the majority of immunoprecipitation reactions. p45 was found to be a proteolytic fragment of p57 by microsequence analysis. Migration of molecular weight standards by SDS-PAGE are indicated on the right.

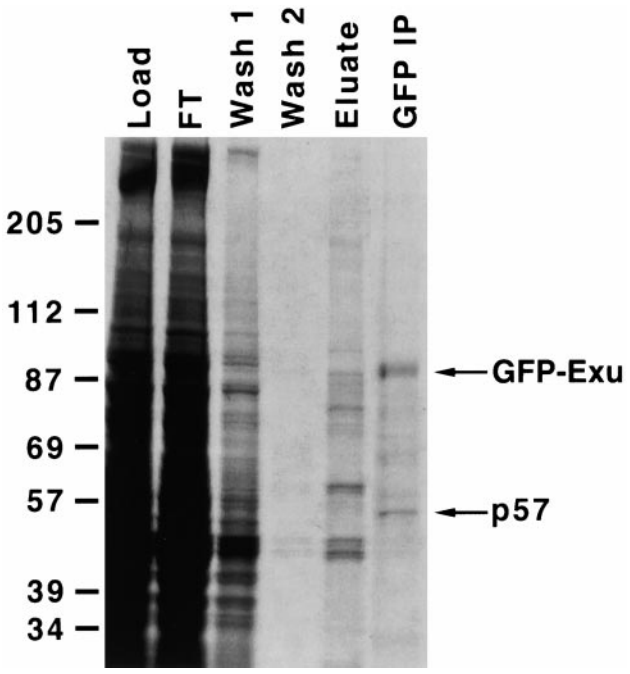

Figure 3. Purification of GFP-Exu-His_6 by metal affinity chromatography and GFP antibody immunoprecipitation. Shown are the initial load, the flow through (FT) from the Ni-NTA column, two wash steps, the imidazole eluate (Eluate), and anti-GFP immunoprecipitation from the Ni-NTA eluate (GFP IP). p57 copurifies with GFP-Exu-His_6 through this procedure. Details of the purification procedures are found in Materials and Methods. Migration of molecular weight standards SDS-PAGE are indicated on the left.

crosequenced three tryptic peptides from the purified protein. The sequence from two of the three peptides matched a previously identified protein, the product of the *yps* gene (Fig. 4 A). Yps is a member of the cold shock family of RNA-binding domain proteins and was identified as part of a degenerate PCR screen to identify cold shock domain containing genes from *Drosophila melanogaster* (Thieringer et al., 1997). However, the third peptide only matched the Yps sequence in a reading frame other than the published open reading frame. To rule out the possibility that *yps* expression is subject to ribosomal frameshifting or RNA editing, we obtained and sequenced six independent *yps* ESTs (Berkeley *Drosophila* Genome Project/Howard Hughes Medical Institute EST Project, unpublished). Our sequence revealed that the original *yps* sequence contained several sequencing errors and that the correct open reading frame contains all three microsequenced peptides (Fig. 4 A). The cold shock domain of Yps shows extensive sequence identity to other cold shock domain proteins (Fig. 4 B). This domain has been shown in several studies to bind RNA, although its ability to recognize specific substrates remains uncertain (Murray, 1994; Bouvet et al., 1995; Matsumoto et al., 1996). Beyond the cold shock domain, Yps exhibited no significant homology to any other protein except YB-1, a cold shock domain protein from *Drosophila silvesteris* (AAC06034).

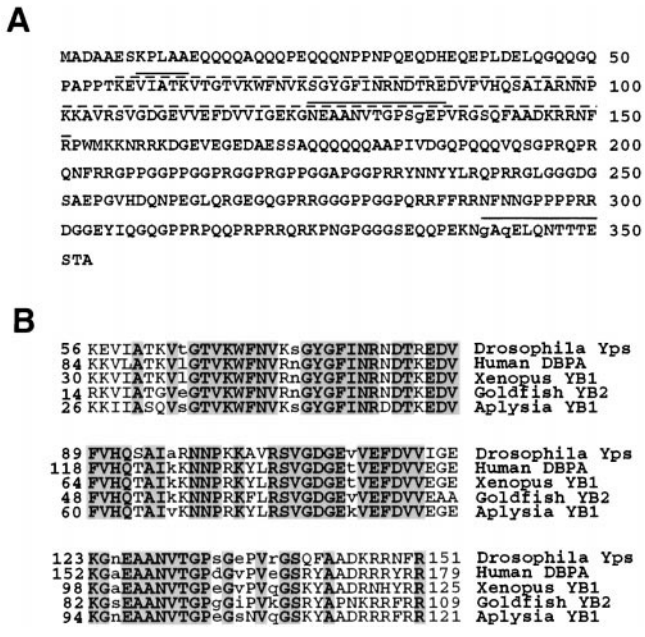

Figure 4. Sequence of p57/Yps, a cold shock domain RNA binding protein. (A) The predicted protein sequence of Yps determined from sequencing of six ESTs from the Berkeley *Drosophila* Genome Project. Solid lines highlight the peptides obtained by microsequencing of p57. Mismatches between the translated sequence and the microsequenced peptides are in lower case. The dashed line delineates the cold shock domain. Amino acid residue number are shown on the right. (B) Sequence alignment of the cold shock domain of Yps with other cold shock domains from human (DBPA), Xenopus (YB1), goldfish (YB2), and Aplysia (YB1) proteins. Residues that are identical in all five proteins are highlighted. Residues that are identical or similar in four of the five proteins are shown in upper case and less well-conserved residues are in lower case.

Since the YB-1 protein is 70% identical to Yps across the entire length of the protein, it is likely to be a true ortholog of Yps. No function was assigned to either YB-1 or Yps in these prior studies.

Yps Is a Component of the Exu Complex

To further characterize Yps, we prepared affinity purified antibodies against bacterially expressed Yps (amino acids 1–160). These antibodies recognized the 57-kD Yps protein in crude extracts by immunoblot (Fig. 5 A). Using the Yps antibody, we found that Yps comigrates with Exu in sucrose gradients and is distributed broadly in the 20–60 S size range (Fig. 5 B). To rule out the possibility that Exu and Yps are components of distinct complexes of similar size, GFP-Exu was immunoprecipitated from individual gradient fractions and immunoblotted with the Yps antibody (Fig. 5 C). This experiment showed that Exu and Yps coimmunoprecipitate together across the gradient, arguing strongly that Exu and Yps are part of the same complex.

To provide further evidence for an Exu–Yps complex, we immunoprecipitated GFP-Exu extracts with our anti-Yps polyclonal antibody. In agreement with our previous immunoprecipitation results, immunoblots showed that GFP-Exu specifically coimmunoprecipitates with Yps (Fig. 5 D). However, immunoblots showed only a weak GFP-Exu band in the Yps immunoprecipitate. The inefficient coimmunoprecipitation of GFP-Exu with Yps is probably due to the fact that our anti-Yps antibody may displace Exu from the complex, since it was raised against the Exu-binding region of Yps (discussed below; Fig. 6). The Yps immunoprecipitates also contained the same six proteins (p74, p76, p78, p82, p88, and p147) that strongly coimmunoprecipitated with GFP-Exu and were present in similar stoichiometries (Fig. 5 E). The coimmunoprecipitation of these six proteins with Yps was diminished by RNase treatment, as was observed in our previous Exu immunoprecipitation experiments (Fig. 5 E). The ability of Yps and Exu antibodies to coimmunoprecipitate the same set of polypeptides argues that these proteins are bona fide components of the Exu-Yps complex.

Exuperantia Binds Directly to the NH_2-Terminal Region of Yps in the Absence of RNA or Other Proteins

The coimmunoprecipitation of Exu and Yps after RNase A treatment suggested, but did not prove, that Exu and Yps bound directly to each other. To test this idea, we examined the Exu–Yps interaction in an in vitro translation reaction (Fig. 6). Myc-tagged Yps was in vitro translated in the presence of [^{35}S]methionine and then added to an unlabeled in vitro translation of HA-tagged Exu. Before mixing, each translation reaction was treated with RNase A to eliminate any residual RNA from the translation reaction. When HA–Exu was immunoprecipitated from the combined mixture with the anti-HA antibody, the ^{35}S-labeled myc-Yps protein was coimmunoprecipitated. The amount of myc-Yps that coimmunoprecipitated with HA–Exu was approximately half of the amount of myc-Yps that was immunoprecipitated directly with the anti-myc antibody, showing that Yps is predominantly bound to Exu under these experimental conditions. These results demonstrate that the additional RNA and protein components of the

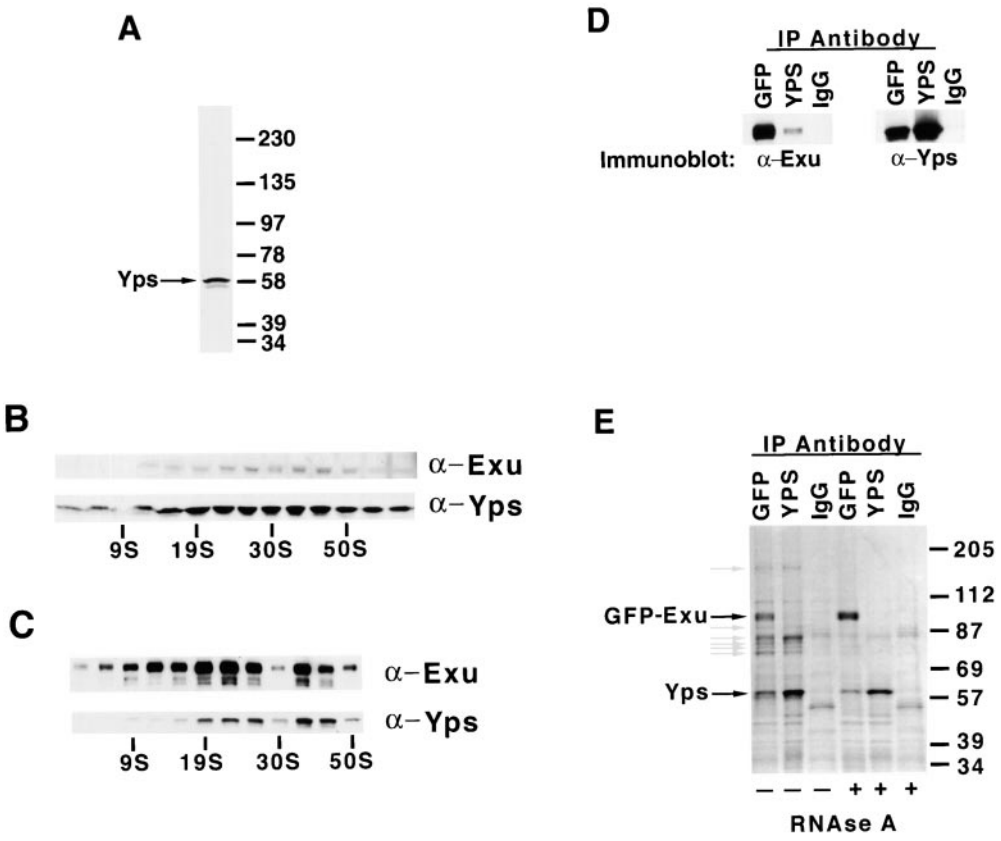

Figure 5. Yps sedimentation and identification of associated proteins. (A) Immunoblot of total fly extract with affinity purified anti-Yps antibody. Migration of molecular weight standards by SDS-PAGE are indicated. (B) Sedimentation of Exu and Yps in extracts made from frozen GFP-Exu expressing flies through a 5–40% sucrose gradient. Both Exu and Yps, detected by immunoblot, sediment broadly with the peak centered at 25–30 S. (C) Immunoblot of Exu and Yps in anti-GFP immunoprecipitations of a 5–40% sucrose density gradient loaded with extract made from frozen GFP-Exu expressing flies. Both Exu and Yps coimmunoprecipitate together across the gradient, indicating that they are both part of the same complex. The decrease in signal in the fraction at 30 S is due to poor recovery from that immunoprecipitation reaction. (D) Immunoblot for Exu and Yps in immunoprecipitates from GFP-Exu extract using anti-GFP (GFP), anti-Yps (YPS), or rabbit IgG (IgG) antibodies. Exu coimmunoprecipitates with Yps, although the signal is not as robust as the Exu signal in the anti-GFP immunoprecipitation. This is likely due to the fact that the anti-Yps antibody was raised against the Exu binding region of Yps and hence, may displace Exu from the complex. (E) Coomassie-stained SDS-PAGE gel of immunoprecipitates from GFP-Exu fly extracts using anti-GFP, anti-Yps, or rabbit IgG antibodies. Dark arrows indicate GFP-Exu and Yps. Grey arrows indicate the six polypeptides that are present in both anti-GFP and anti-Yps immunoprecipitates, but are absent from both immunoprecipitates when RNase-treated extracts are used (see Materials and Methods). Migration of molecular weight standards by SDS-PAGE are indicated.

native Exu complex are not required for Exu and Yps to associate stably with each other (Fig. 6).

To determine which region of Yps is important for binding to Exu, deletions of myc-Yps were assayed for their ability to bind HA–Exu in vitro. The NH_2-terminal region (1–160 amino acids) of Yps, which contains the cold shock domain, bound to Exu at the same efficiency as the full-length protein (Fig. 6). However, the minimal cold shock domain (56–151 amino acids) did not bind to Exu in this assay (Fig. 6), suggesting that the sequences flanking the cold shock domain are likely to contribute to the Exu-binding site. The proline-rich COOH terminus of Yps presumably is not sufficient for binding. However, this could not be assessed experimentally, since this region did not stably express either in vitro or in bacteria.

osk mRNA Is Present in the Exu–Yps Complex

The shift in the size of the Exu–Yps complex after RNase treatment suggested that it might be directly involved in mRNA localization. To test this idea, we immunoprecipitated either Exu or Yps from extracts and analyzed the pellet for the presence of various localized (*bcd*, *osk*, *nos*) messages and a housekeeping message (*phosphoglycerokinase* [*pgk*]). We analyzed these four transcripts because each gene appears in the EST database (Berkeley *Drosophila* Genome Project/Howard Hughes Medical Institute EST Project, unpublished) at roughly equivalent frequencies, indicating that these messages are likely to be present in comparable amounts. Furthermore, *bcd*, *osk*, and *nos* are localized differently during oogenesis. *bcd* mRNA is localized to the anterior of the oocyte beginning at stage 7 of oogenesis; *osk* mRNA is localized transiently to the anterior of the oocyte during stages 8/9 and is exclusively localized to the posterior by the end of stage 9; *nos* mRNA is localized to the posterior of the oocyte during late oogenesis. Using a RT-PCR assay, we amplified *bcd*, *osk*, *nos*, and *pgk* transcripts from total RNA from extracts (Fig. 7 A). When GFP-Exu immunoprecipitates were analyzed by RT-PCR, *osk* transcript (Fig. 7 B), but none of the others (data not shown) was amplified by RT-PCR. The identical result was obtained when RT-PCR was performed on immunoprecipitations with the anti-Yps antibody, whereas control IgG immunoprecipitations yielded no *osk* RT-PCR signal (Fig. 7 B). To rule out artifacts due to signal saturation, we serially diluted the RT

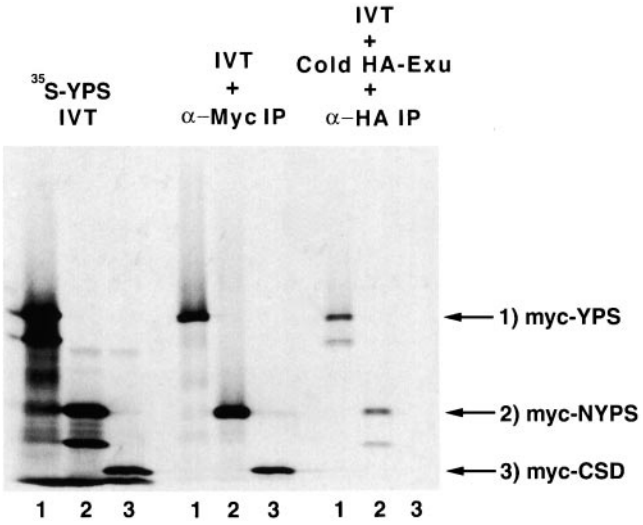

Figure 6. Binding of Exu and Yps in in vitro translation reactions. Autoradiogram of in vitro translation products of myc-tagged Yps (myc-YPS; lane 1); myc-tagged NH_2-terminal Yps, amino acids 1–160, (myc-NYPS; lane 2); and myc-tagged cold shock domain of Yps, amino acids 56–151, (myc-CSD; lane 3). Shown are the in vitro translation products (^{35}S-YPS IVT), immunoprecipitations with the anti-myc antibody (IVT + α-Myc IP), and anti-HA immunoprecipitations of unlabeled HA-tagged Exu mixed with ^{35}S-labeled in vitro translations (IVT + Cold HA–Exu + α-HA IP). The lower band present in the in vitro translation and cold HA–Exu reactions is a proteolytic product of Yps, since it is not present in our anti-myc immunoprecipitations of Yps. These experiments show that Exu binds directly to the NH_2-terminal domain of Yps.

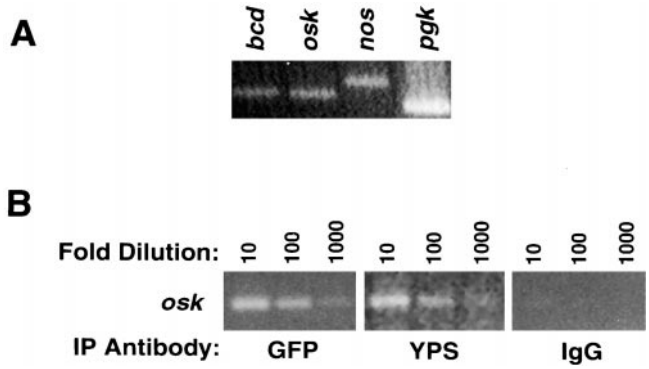

Figure 7. Amplification of *osk* mRNA by RT-PCR from the Exu-Yps complex. (A) RT-PCR of *bcd*, *osk*, *nos*, and *pgk* from 5 μg of total mRNA isolated from GFP-Exu extracts. All transcripts are easily detected in total mRNA. (B) RT-PCR using *osk*-specific primers from RNA isolated from immunoprecipitates of GFP-Exu fly extract using anti-GFP, anti-Yps, or rabbit IgG. The RT reaction was diluted 10-, 100-, or 1,000-fold before the PCR step. In contrast to the signal observed with *osk* primers, *bcd*, *nos*, and *pgk* primers did not amplify any detectable signal from the same material (data not shown). Details of this procedure are found in Materials and Methods.

product from our immunoprecipitations before conducting the PCR. *osk* mRNA was consistently detected in the 10-, 100-, and 1,000-fold dilutions of the RT product, and the signal decreased with increasing dilution (Fig. 7 B). This result indicates that the PCR reaction is approximately in the linear range and that signal saturation is not a factor in our assay. Therefore, the RT-PCR assay demonstrates that both Yps and Exu are associated with a complex that contains *osk* mRNA. This was an unanticipated result, since previous genetic studies only reported a role for *exu* in the localization of *bcd* mRNA to the anterior of the oocyte. We cannot rule out that the Exu–Yps complex contains *bcd* mRNA, since our negative result could reflect technical difficulties, such as poor *bcd* mRNA stability. However, our RT-PCR results suggested the unanticipated possibility that *exu* is involved in posterior mRNA localization.

Yps Colocalizes with Exu in Oocytes and Nurse Cells and Accumulates at the Posterior Pole during Mid-Oogenesis

To learn more about the in vivo role of Yps in RNA localization, *Drosophila* ovaries were labeled with affinity purified antibodies to the NH_2 terminus (1–160 amino acids) of Yps. Immunofluorescence staining revealed a strong Yps signal in both the germ cells and follicle cells of developing egg chambers (Fig. 8). In contrast, labeling with secondary antibody alone produced a much weaker background signal (data not shown). This result, together with the specificity of our anti-Yps antibody by immunoblot (Fig. 5 A), argues that the staining we observe is specific for Yps. Examination of different stage egg chambers (for staging see Spradling, 1993) revealed that Yps accumulates in the oocyte during stages 1–7. This signal was stronger at the posterior of the oocyte in early stages, although it was also present throughout much of the oocyte cytoplasm (Fig. 8 A). In both early and midstage egg chambers, Yps exhibited a particulate staining that was frequently concentrated around the nurse cell nuclei (Fig. 8 B). At stages 8 and 9, faint anterior localization was sometimes apparent in the oocyte (Fig. 8 C), and during stages 9 and 10 Yps accumulated at the posterior of the oocyte (Fig. 8, C and D).

The localization of Yps during oogenesis was very similar to the previously observed distribution of GFP-Exu (Wang and Hazelrigg, 1994). To compare the distributions of Exu and Yps directly, we immunostained Yps in egg chambers expressing GFP-Exu. Individual particles containing both proteins were detected in the nurse cells (Fig. 8, E and F). The early accumulation of Yps in the oocyte (stages 1–7), its accumulation at the oocyte anterior (stages 8 and 9), and its later localization to the posterior pole (stages 9 and 10) all coincide with the localization of Exu protein and *osk* mRNA (Ephrussi et al., 1991; Kim-Ha et al., 1991; Wang and Hazelrigg, 1994). The agreement between our biochemical and in vivo localization studies further supports a role for the Exu–Yps complex in the localization of *osk* mRNA. This hypothesis was tested directly by genetic studies, as described below.

exu Mutants Have Defects in osk mRNA Localization

Whole mount in situ hybridization was performed on ovaries from wild-type (Oregon R) and *exu* null (*exu*^{SCO2}/Df[2R]MK1) females to determine whether *exu* is re-

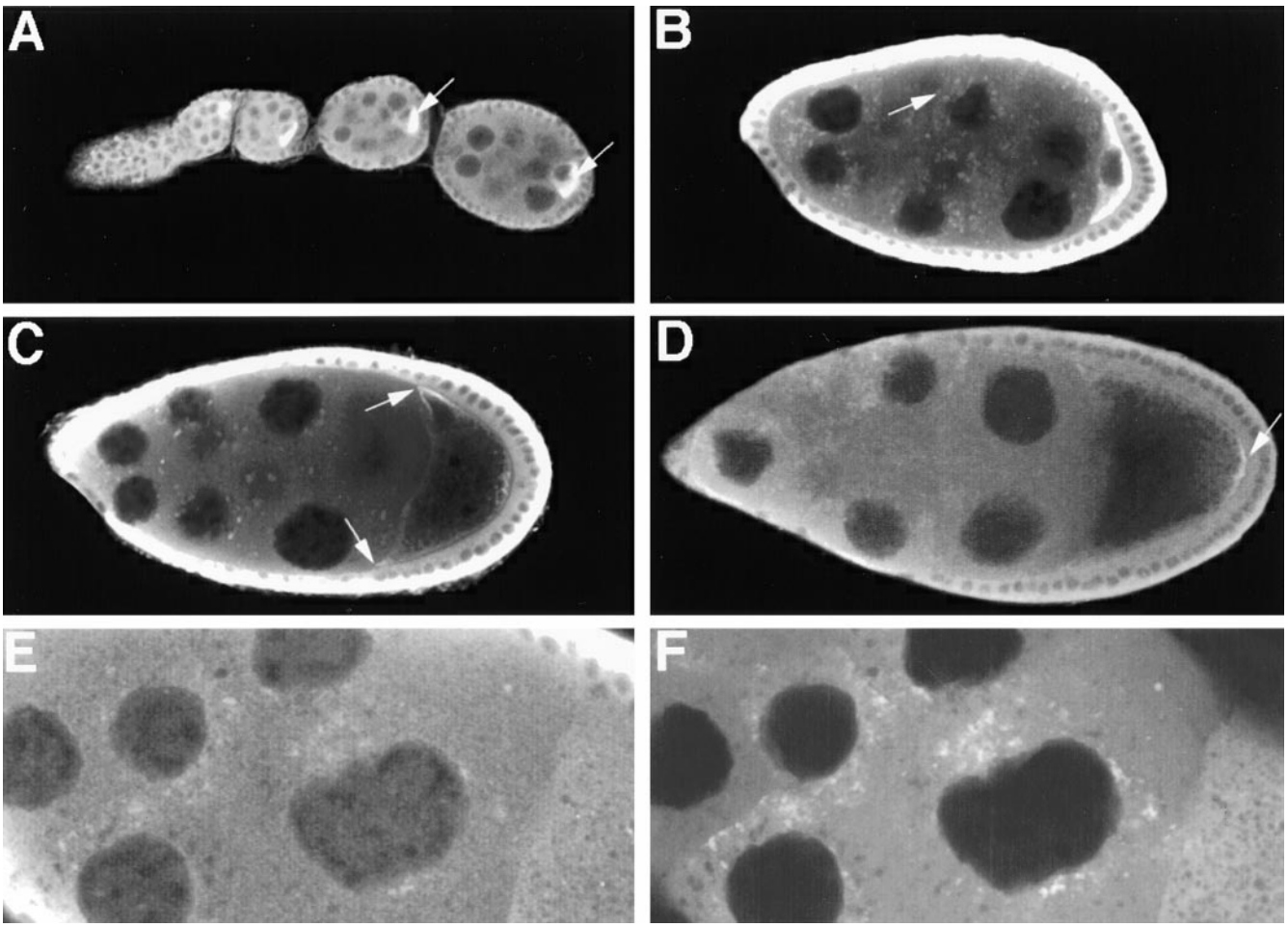

Figure 8. Yps accumulates at the posterior pole during mid-oogenesis and colocalizes with Exu within the ovary. Wild-type (Oregon R) ovaries were labeled with anti-Yps antibody (see Materials and Methods). (A) In previtellogenic stages, Yps is most concentrated in the oocyte (arrows). (B) In both early and midstage egg chambers, Yps is present in particles that cluster around the nurse cell nuclei (arrow). (C) At stage 9, Yps continues to be concentrated in particles in the nurse cell cytoplasm, while it begins to accumulate at the posterior pole and anterior margin (arrows) of the oocyte. (D) During stage 9, Yps is restricted to the posterior pole of the oocyte (arrow). Yps is also highly expressed in the follicle cells, the somatic cells that surround each egg chamber, during all stages of oogenesis, although this is not visible in all images due to the plane of focus. For colocalization studies (E and F), ovaries from flies carrying a *gfp-exu* transgene were labeled with an anti-Yps antibody detected with a rhodamine-tagged secondary antibody. (E) In the nurse cells of a stage 10 egg chamber, Yps is localized to perinuclear particles that colocalize with (F) GFP-Exu particles.

quired for any aspect of *osk* mRNA localization. In ovaries from wild-type females, *osk* mRNA is often concentrated in apical patches in the nurse cells of stage 9 and 10 egg chambers (Pokrywka and Stephenson, 1995) (Fig. 9 A). In contrast, *osk* mRNA was dispersed in the nurse cells of *exu* egg chambers of the same stages (Fig. 9 B). Thus, *exu* is required for *osk* mRNA to be correctly localized within nurse cells. Interestingly, *bcd* mRNA is also localized to apical patches in the nurse cells in an *exu*-dependent manner (St Johnston et al., 1989). Although the functional significance of this nurse cell localization is unknown, the fact that *exu* mutants disrupt this localization for both *osk* and *bcd* mRNAs indicates that at least some of the components required for this localization are common to both transcripts.

exu mutants also caused a partial defect in *osk* mRNA localization to the posterior pole. In ovaries from wild-type females, a strong *osk* mRNA signal was detected at the posterior pole in 90% ($n = 90$) of wild-type stage 9 and stage 10 oocytes (Fig. 9 C); the remainder (10%) showed reduced (9%) or barely detectable (1%) posterior *osk* mRNA signal. In contrast, only 64% of stage 9 and stage 10 egg chambers from *exu* mutants ($n = 210$) showed an *osk* mRNA signal at the posterior of the oocyte, and this signal was consistently weaker than that observed in the wild-type egg chambers; the remainder (36%) showed reduced (23%), barely detectable (8%) (Fig. 9 D), or no (5%) posterior *osk* mRNA signal. Thus, mutations in *exu* cause a defect in the amount of *osk* mRNA that is localized to the posterior pole during stages 9 and 10 of oogenesis.

Discussion

Although mRNA localization in *Drosophila* has been the subject of extensive genetic analysis, only a few attempts have been made to characterize biochemically the proteins

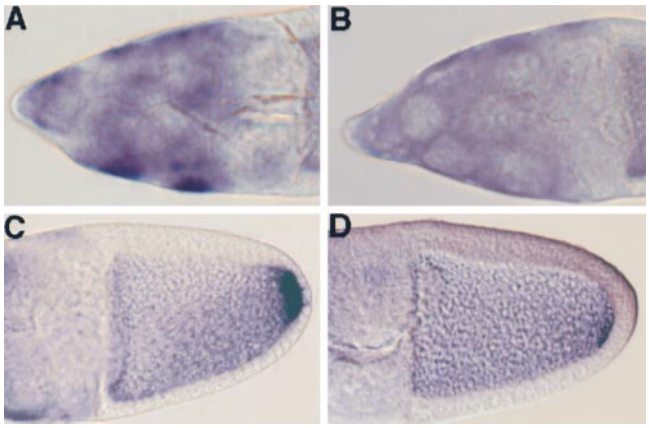

Figure 9. osk mRNA localization is disrupted in *exu*^{SCO2} egg chambers. Whole mount in situ hybridization was performed on egg chambers from wild-type (Oregon R) and *exu*^{SCO2} flies raised at 18°C to examine the distribution of *osk* mRNA. (A) In the nurse cells of wild-type stage 10 egg chambers, *osk* mRNA is often concentrated in patches within the nurse cell cytoplasm. (B) In nurse cells from stage 10 *exu*^{SCO2}/Df(2R)MK1 egg chambers, the *osk* mRNA signal within the nurse cells is frequently dispersed. (C) In oocytes from wild-type stage 10 egg chambers, *osk* mRNA is highly concentrated at the posterior pole. (D) In oocytes from stage 10 *exu*^{SCO2}/Df(2R)MK1 egg chambers, the *osk* mRNA signal is often reduced at the posterior pole. This particular egg chamber is an example of an oocyte with barely detectable *osk* mRNA (see text).

associated with localized messages. In this study, we have demonstrated that Exu, a protein shown by genetic studies to be involved in mRNA localization, is part of a large RNase-sensitive complex. Through a combination of affinity chromatography and immunoprecipitation experiments, we have uncovered seven proteins associated with the Exu complex, one of which is a new RNA-binding protein, Yps.

To our knowledge, this is the first isolation of a native RNP complex involved in RNA localization. There are several pieces of evidence that argue against the Exu-containing complex being a biochemical artifact. First, the complex was identified using three different antibodies for immunoprecipitation. Second, the complex that we isolated from total fly homogenates is not an artifact of mixing proteins from different tissues, since it is also present in extracts made from hand dissected ovaries. Third, Exu and Yps also copurified after metal affinity chromatography, and the two proteins interact in vitro in the absence of RNA. Fourth, Exu and Yps colocalize by immunofluorescence indicating that they form a complex in vivo. Fifth, Exu, Yps, and *osk* mRNA all show a transitory accumulation at the anterior in mid-oogenesis and then colocalize at the posterior pole. Finally, the relevance of the biochemical association with *osk* mRNA is supported by genetic experiments showing a mislocalization of *osk* mRNA in *exu*-null mutants. Although further genetic analysis of Yps and the other proteins in the complex will provide additional insights into this problem, the current combination of biochemical cofractionation, in vivo colocalization, and genetic analysis argues for a direct role of Exu and its associated proteins in mRNA localization.

The Role of the Exu Complex in mRNA Localization

Previous genetic work implicated *exu* in mRNA localization, but did not address whether Exu plays a direct or indirect role in the localization process (Berleth et al., 1988; St Johnston et al., 1989; Macdonald et al., 1991; Marcey et al., 1991). This study supports a direct involvement for Exu, since we show that Exu is part of a large RNase-sensitive complex and interacts directly with an RNA-binding protein. Furthermore, the association of *osk* mRNA with the Exu complex establishes a physical connection between Exu and a localized mRNA. The biochemical characteristics of our large Exu complex also likely reflect the properties of Exu in vivo. Exu has been shown to be part of large particles by both GFP fluorescence (Wang and Hazelrigg, 1994) and immunoelectron microscopy (Wilsch-Brauninger et al., 1997). Moreover, Exu and Yps, which are associated components in our biochemically isolated complex, also colocalize in particles within the nurse cells and oocytes.

The identification of *osk* mRNA in the Exu–Yps complex was surprizing, given the pronounced anterior patterning defects associated with *exu* mutants (Schupbach and Wieschaus, 1986). However, a role for Exu in *osk* mRNA localization is consistent with several other findings. First, previous work has shown that Exu accumulates at both the anterior and posterior poles of the oocyte (Marcey et al., 1991; Wang and Hazelrigg, 1994). Second, *osk* mRNA transiently accumulates at the anterior pole along with *bcd* mRNA before its transport to the posterior (Ephrussi et al., 1991; Kim-Ha et al., 1991). Finally, one of the effects of *exu* mutants was to disrupt the localization of *osk* mRNA to apical patches within nurse cells. This defect is identical to the nurse cell localization defect described previously for *bcd* mRNA in *exu* mutants (St Johnston et al., 1989) and suggests that this step in the localization pathway may be common to both transcripts.

One of the reasons that *exu* mutants have not been examined previously for defects in *osk* mRNA localization is that only a small percentage of embryos from *exu* mothers display posterior patterning defects (Schupbach and Wieschaus, 1986). Our examination of *exu* mutants revealed that the amount of *osk* mRNA localized to the posterior pole is decreased in these mutants, suggesting that *exu* plays a role in localizing *osk* mRNA within oocytes. However, as this defect is only partially penetrant, Exu-dependent posterior localization within the oocyte may be redundant with other localization mechanisms. In addition, the posterior patterning defects associated with the decrease in *osk* mRNA localization in *exu* mutants during stages 9 and 10 of oogenesis may be rescued by localization of *osk* mRNA during cytoplasmic streaming later in oogenesis. In support of this idea, Glotzer et al. (1997) have shown that injected, fluorescently labeled *osk* mRNA can be localized to the posterior at the time when cytoplasmic streaming occurs. Such localization most likely occurs by random motion during cytoplasmic streaming and specific anchoring of *osk* mRNAs that come in contact with the posterior pole. These multiple mechanisms of localizing *osk* mRNA account for the fact that *exu* mutants do not display pronounced defects in abdominal patterning.

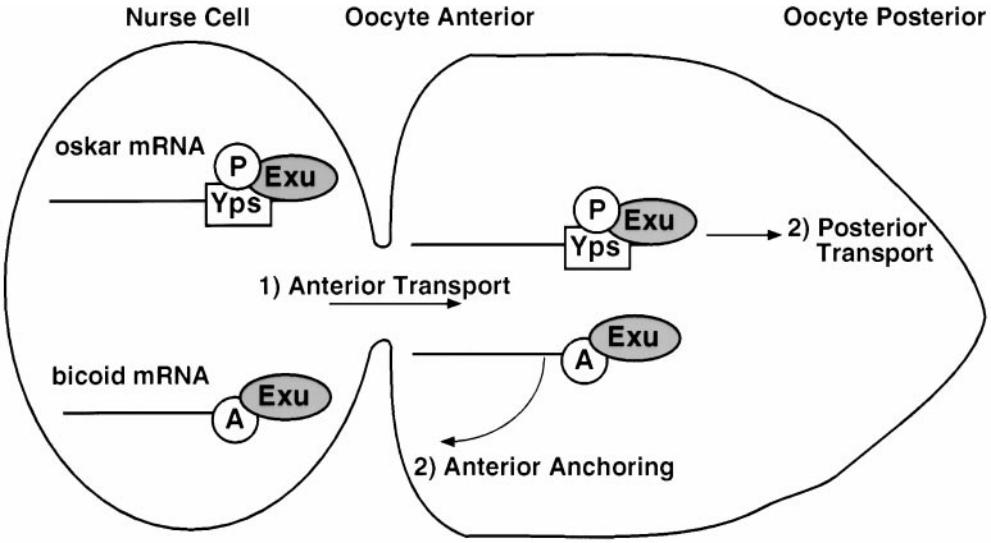

Figure 10. A two-step model for sorting mRNAs to the anterior and posterior poles of the oocyte. *osk* and *bcd* mRNAs each recruit transcript-specific proteins (A and P) as well as common components, such as Exu. Exu is involved in transport of *osk* and *bcd* mRNAs from the nurse cells to the anterior of the oocyte (step 1). Once at the anterior, the specific components (A and P) sort mRNAs so that *bcd* mRNA is anchored to the anterior of the oocyte, while *osk* mRNA is transported to the posterior. In this model, we have depicted Yps as a candidate component of *osk* mRNA-specific complexes for reasons described in the text.

Previous work has shown that *exu* is necessary for normal *bcd* mRNA localization (Berleth et al., 1988; St Johnston et al., 1989; Pokrywka and Stephenson, 1991; Macdonald and Kerr, 1997), although these studies did not establish a direct connection between Exu and *bcd* mRNA. Nevertheless, it was surprising that we could not detect *bcd* mRNA in our Exu complex. This negative result should not be taken to indicate that *bcd* mRNA is not in the complex, since it could reflect poor stability of *bcd* mRNA, a weaker association of *bcd* mRNA with the Exu complex, or difficulty in extracting and/or purifying RNP particles containing *bcd* mRNA. Alternatively, it is possible that *exu*'s role in *bcd* localization is indirect. We are currently trying to address these issues by using other approaches to detect specific Exu–*bcd* mRNA interactions.

The Role of Yps in mRNA Localization

Our biochemical studies linking Yps to Exu and *osk* mRNA suggest that this RNA-binding protein plays a role in posterior mRNA localization. This assertion is further supported by our immunofluorescence studies showing that Yps and *osk* mRNA have strikingly similar localization patterns throughout oogenesis: both accumulate in the early oocyte, transiently localize to the oocyte anterior during stages 8 and 9, and then assume their final positions at the posterior pole during stages 9 and 10 (Fig. 8) (Ephrussi et al., 1991; Kim-Ha et al., 1991). What role might Yps play in the localization complex? Yps belongs to the cold shock domain family of RNA-binding proteins that have been implicated previously in regulating translation and mRNA secondary structure (Jiang et al., 1997; Sommerville, 1999). A notable example is FRGY2, which is complexed with mRNAs in the *Xenopus* oocyte and is thought to be important for translational silencing (Tafuri and Wolffe, 1993; Yurkova and Murray, 1997). Yps may serve a similar role, since *osk* mRNA is translationally repressed until it reaches the posterior pole (Kim-Ha et al., 1995; Macdonald and Smibert, 1996; Gunkel et al., 1998). Interestingly, Yps must also serve a function without Exu, since *yps* is expressed broadly, whereas *exu* expression is limited to the germ line (Macdonald et al., 1991; Marcey et al., 1991; Thieringer et al., 1997). It is possible that Yps is a component of the mRNA localization machinery outside the germ line, since other components of the oocyte mRNA localization machinery, such as Staufen, are also used for mRNA localization in somatic tissues (Li et al., 1997; Broadus et al., 1998). Determining Yps's precise involvement in transport and/or translational regulation in the oocyte and other tissues will be resolved in the future by mutational studies.

A Model for mRNA Transport by the Exu–Yps Complex

The pathways by which anterior- and posterior-localized mRNAs arrive at their destinations are poorly understood, although it is generally believed that these RNAs are recognized by different proteins and utilize distinct transport machineries. However, we propose that anterior- and posterior-localized mRNAs begin their localization process in the nurse cells using a similar complex, with Exu serving as a common core component (Fig. 10). In our model, one of Exu's functions is as a component of an mRNA transport complex, since GFP-Exu particles have been observed to move in a microtubule-dependent manner (Theurkauf and Hazelrigg, 1998). Consistent with this idea, both *osk* and *bcd* mRNA accumulate in apical patches within nurse cells, and *exu* mutants disrupt this localization pattern for both mRNAs (St Johnston et al., 1989; Pokrywka and Stephenson, 1995) (Fig. 9 B). We also propose that the Exu complex transports mRNAs from the nurse cells to the oocyte as well as within the oocyte (Fig. 10), although these transport steps also can be achieved through other redundant mechanisms, such as nurse cell dumping and cytoplasmic streaming (Spradling, 1993). Although the above model places Exu as part of a transport complex, it

should be noted that our present data also could be explained if Exu contributes to the establishment of anchoring once mRNAs reach their final destination.

After arriving in the oocyte, *bcd*- and *osk*-containing RNPs must be sorted so that *bcd* becomes anchored at the anterior, whereas *osk* is transported to the posterior pole. Since Yps, Exu, *bcd* mRNA, and *osk* mRNA all first colocalize at the anterior (Fig. 8) (Ephrussi et al., 1991; Kim-Ha et al., 1991; Wang and Hazelrigg, 1994; Theurkauf and Hazelrigg, 1998), we propose that this sorting decision occurs at the anterior of the oocyte (Fig. 10). Evidence for this anterior sorting model comes from genetic studies of *staufen* (*stau*) and *tropomyosin II* (*TmII*), which show that these proteins do not interfere with anterior localization but rather block the release and transport of *osk* transcripts to the posterior (Ephrussi et al., 1991; Kim-Ha et al., 1991; Erdelyi et al., 1995; Tetzlaff et al., 1996). The molecular basis for this sorting decision is unclear, but may involve modifications to the transport machinery or the recruitment of additional factors.

Biochemistry of the Exu Complex: Relationship to In Vivo Function

Biochemical isolation of a native RNP complex provides an opportunity to identify new proteins involved in mRNA localization, which may have been missed by genetic analyses due to lethality or redundant functions. However, a significant caveat of our approach is that our isolated RNP particles may be heterogeneous, since our purification strategy begins with a crude extract containing material from egg chambers at all stages of oogenesis. Thus, it is likely that our biochemically-isolated material may represent a spectrum of complexes that comprise transport intermediates from the recognition of localized mRNAs in the nurse cells to the anchoring of the complexes at the posterior poles. In addition to temporal changes in the composition of the Exu complex, it is also possible that multiple Exu particles exist which contain distinct mRNA cargos.

To resolve these important issues, it will be important to determine the molecular identity of the six RNase-sensitive polypeptides in our Exu complex and determine if they are required selectively for the localization of *bcd* mRNA or *osk* mRNA. In addition, simultaneous observation and colocalization of GFP-tagged mRNAs (Bertrand et al., 1998) and blue fluorescent protein–tagged protein components of the Exu complex will reveal which mRNAs and polypeptides are contained within the same transport complex in vivo. This approach will also allow direct observation of mRNA transport in *Drosophila* for the first time and provide a method for analyzing the changes in RNP components during the movement of RNAs from the nurse cell to their final destination in the oocyte.

We thank Erin O'Shea, Joachim Li, and Vishu Lingappa for providing plasmids for in vitro translation studies, and Dave Morgan for providing the anti-HA antibody. We also thank Paul MacDonald for generously providing the anti-Exu antibody and much helpful advice. We are grateful to Dara Friedman and Maki Inada for critically reading the manuscript and the members of the Vale lab for helpful discussions.

This work was supported in part by grants from the National Institutes of Health (GM48499) to R.D. Vale and the National Institutes of Health (GM48060) and National Science Foundation (IBN-98-17089) to T. Hazelrigg. J.E. Wilhelm was supported by the Medical Scientist Training Program.

Submitted: 20 October 1999
Revised: 10 December 1999
Accepted: 15 December 1999

References

Ainger, K., D. Avossa, F. Morgan, S.J. Hill, C. Barry, E. Barbarese, and J.H. Carson. 1993. Transport and localization of exogenous myelin basic protein mRNA injected into oligodendrocytes. *J. Cell Biol.* 123:431–441.

Bashirullah, A., R.L. Cooperstock, and H.D. Lipshitz. 1998. RNA localization in development. *Annu. Rev. Biochem.* 67:335–394.

Bassell, G., and R.H. Singer. 1997. mRNA and cytoskeletal filaments. *Curr. Opin. Cell Biol.* 9:109–115.

Berleth, T., M. Burri, G. Thoma, D. Bopp, S. Richstein, G. Frigerio, M. Noll, and C. Nusslein-Volhard. 1988. The role of localization of bicoid RNA in organizing the anterior pattern of the Drosophila embryo. *EMBO (Eur. Mol. Biol. Organ.) J.* 7:1749–1756.

Bertrand, E., P. Chartrand, M. Schaefer, S.M. Shenoy, R.H. Singer, and R.M. Long. 1998. Localization of ASH1 mRNA particles in living yeast. *Mol. Cell.* 2:437–445.

Bouvet, P., K. Matsumoto, and A.P. Wolffe. 1995. Sequence-specific RNA recognition by the *Xenopus* Y-box proteins. An essential role for the cold shock domain. *J. Biol. Chem.* 270:28297–28303.

Breitwieser, W., F.H. Markussen, H. Horstmann, and A. Ephrussi. 1996. Oskar protein interaction with Vasa represents an essential step in polar granule assembly. *Genes Dev.* 10:2179–2188.

Broadus, J., S. Fuerstenberg, and C.Q. Doe. 1998. Staufen-dependent localization of prospero mRNA contributes to neuroblast daughter-cell fate. *Nature.* 391:792–795.

Cote, C.A., D. Gautreau, J.M. Denegre, T.L. Kress, N.A. Terry, and K.L. Mowry. 1999. A *Xenopus* protein related to hnRNP I has a role in cytoplasmic RNA localization. *Mol. Cell.* 4:431–437.

Deshler, J.O., M.I. Highett, and B.J. Schnapp. 1997. Localization of *Xenopus* Vg1 mRNA by Vera protein and the endoplasmic reticulum. *Science.* 276: 1128–1131.

Ephrussi, A., L.K. Dickinson, and R. Lehmann. 1991. Oskar organizes the germ plasm and directs localization of the posterior determinant nanos. *Cell.* 66: 37–50.

Erdelyi, M., A.M. Michon, A. Guichet, J.B. Glotzer, and A. Ephrussi. 1995. Requirement for *Drosophila* cytoplasmic tropomyosin in oskar mRNA localization. *Nature.* 377:524–527.

Ferrandon, D., L. Elphick, C. Nusslein-Volhard, and D. St Johnston. 1994. Staufen protein associates with the 3′UTR of bicoid mRNA to form particles that move in a microtubule-dependent manner. *Cell.* 79:1221–1232.

Gavis, E.R. 1997. Expeditions to the pole: RNA localization in *Xenopus* and *Drosophila*. *Trends Cell Biol.* 7:485–492.

Glotzer, J.B., R. Saffrich, M. Glotzer, and A. Ephrussi. 1997. Cytoplasmic flows localize injected oskar RNA in *Drosophila* oocytes. *Curr. Biol.* 7:326–337.

Gunkel, N., T. Yano, F.H. Markussen, L.C. Olsen, and A. Ephrussi. 1998. Localization-dependent translation requires a functional interaction between the 5′ and 3′ ends of oskar mRNA. *Genes Dev.* 12:1652–1664.

Havin, L., A. Git, Z. Elisha, F. Oberman, K. Yaniv, S.P. Schwartz, N. Standart, and J.K. Yisraeli. 1998. RNA-binding protein conserved in both microtubule- and microfilament-based RNA localization. *Genes Dev.* 12:1593–1598.

Hazelrigg, T. 1998. The destinies and destinations of RNAs. *Cell.* 95:451–460.

Hellman, U., C. Wernstedt, J. Gonez, and C.H. Heldin. 1995. Improvement of an "In-Gel" digestion procedure for the micropreparation of internal protein fragments for amino acid sequencing. *Anal. Biochem.* 224:451–455.

Hoek, K.S., G.J. Kidd, J.H. Carson, and R. Smith. 1998. hnRNP A2 selectively binds the cytoplasmic transport sequence of myelin basic protein mRNA. *Biochemistry.* 37:7021–7029.

Jiang, W., Y. Hou, and M. Inouye. 1997. CspA, the major cold-shock protein of *Escherichia coli*, is an RNA chaperone. *J. Biol. Chem.* 272:196–202.

Kim-Ha, J., J.L. Smith, and P.M. Macdonald. 1991. oskar mRNA is localized to the posterior pole of the *Drosophila* oocyte. *Cell.* 66:23–35.

Kim-Ha, J., K. Kerr, and P.M. Macdonald. 1995. Translational regulation of oskar mRNA by bruno, an ovarian RNA-binding protein, is essential. *Cell.* 81: 403–412.

Kislauskis, E.H., and R.H. Singer. 1992. Determinants of mRNA localization. *Curr. Opin. Cell Biol.* 4:975–978.

Kobayashi, S., R. Amikura, A. Nakamura, H. Saito, and M. Okada. 1995. Mislocalization of oskar product in the anterior pole results in ectopic localization of mitochondrial large ribosomal RNA in *Drosophila* embryos. *Dev. Biol.* 169:384–386.

Li, P., X. Yang, M. Wasser, Y. Cai, and W. Chia. 1997. Inscuteable and Staufen mediate asymmetric localization and segregation of prospero RNA during *Drosophila* neuroblast cell divisions. *Cell.* 90:437–447.

Macdonald, P.M., and C.A. Smibert. 1996. Translational regulation of maternal mRNAs. *Curr. Opin. Genet. Dev.* 6:403–407.

Macdonald, P.M., and K. Kerr. 1997. Redundant RNA recognition events in bicoid mRNA localization. *RNA*. 3:1413–1420.

Macdonald, P.M., S.K. Luk, and M. Kilpatrick. 1991. Protein encoded by the exuperantia gene is concentrated at sites of bicoid mRNA accumulation in *Drosophila* nurse cells but not in oocytes or embryos. *Genes Dev*. 5:2455–2466.

MacDonald, P.M., A. Leask, and K. Kerr. 1995. exl protein specifically binds BLE1, a bicoid mRNA localization element, and is required for one phase of its activity. *Proc. Natl. Acad. Sci. USA*. 92:10787–10791.

Marcey, D., W.S. Watkins, and T. Hazelrigg. 1991. The temporal and spatial distribution pattern of maternal exuperantia protein: evidence for a role in establishment but not maintenance of bicoid mRNA localization. *EMBO (Eur. Mol. Biol. Organ.) J*. 10:4259–4266.

Matsumoto, K., F. Meric, and A.P. Wolffe. 1996. Translational repression dependent on the interaction of the *Xenopus* Y-box protein FRGY2 with mRNA. Role of the cold shock domain, tail domain, and selective RNA sequence recognition. *J. Biol. Chem*. 271:22706–22712.

Murray, M.T. 1994. Nucleic acid-binding properties of the *Xenopus* oocyte Y box protein mRNP3+4. *Biochemistry*. 33:13910–13917.

Oleynikov, Y., and R.H. Singer. 1998. RNA localization: different zipcodes, same postman? *Trends Cell Biol*. 8:381–383.

Pokrywka, N.J., and E.C. Stephenson. 1991. Microtubules mediate the localization of bicoid RNA during *Drosophila* oogenesis. *Development*. 113:55–66.

Pokrywka, N.J., and E.C. Stephenson. 1995. Microtubules are a general component of mRNA localization systems in *Drosophila* oocytes. *Dev. Biol*. 167: 363–370.

Ross, A.F., Y. Oleynikov, E.H. Kislauskis, K.L. Taneja, and R.H. Singer. 1997. Characterization of a beta-actin mRNA zipcode-binding protein. *Mol. Cell. Biol*. 17:2158–2165.

Schupbach, T., and E. Wieschaus. 1986. Maternal effect mutations altering the anterior-posterior pattern of the *Drosophila* embryo. *Wilhelm Roux's Arch. Dev. Biol*. 195:302–317.

Smith, J.L., J.E. Wilson, and P.M. Macdonald. 1992. Overexpression of oskar directs ectopic activation of nanos and presumptive pole cell formation in *Drosophila* embryos. *Cell*. 70:849–859.

Sommerville, J. 1999. Activities of cold-shock domain proteins in translation control. *Bioessays*. 21:319–325.

Spradling, A.C. 1993. Developmental genetics of oogenesis. *In* The Development of *Drosophila melanogaster*. Vol. 1. Cold Spring Harbor Laboratory Press, Plainview, N.Y. 1–70.

Spradling, A.C., and G.M. Rubin. 1982. Transposition of cloned P elements into *Drosophila* germ line chromosomes. *Science*. 218:341–347.

St Johnston, D. 1995. The intracellular localization of messenger RNAs. *Cell*. 81:161–170.

St Johnston, D., and C. Nusslein-Volhard. 1992. The origin of pattern and polarity in the *Drosophila* embryo. *Cell*. 68:201–219.

St Johnston, D., W. Driever, T. Berleth, S. Richstein, and C. Nusslein-Volhard. 1989. Multiple steps in the localization of bicoid RNA to the anterior pole of the *Drosophila* oocyte. *Development*. 107:13–19.

St Johnston, D., D. Beuchle, and C. Nusslein-Volhard. 1991. Staufen, a gene required to localize maternal RNAs in the *Drosophila* egg. *Cell*. 66:51–63.

Stephenson, E.C., Y.C. Chao, and J.D. Fackenthal. 1988. Molecular analysis of the swallow gene of *Drosophila melanogaster*. *Genes Dev*. 2:1655–1665.

Tafuri, S.R., and A.P. Wolffe. 1993. Selective recruitment of masked maternal mRNA from messenger ribonucleoprotein particles containing FRGY2 (mRNP4). *J. Biol. Chem*. 268:24255–24261.

Tautz, D., and C. Pfeifle. 1989. A non-radioactive in situ hybridization method for the localization of specific RNAs in *Drosophila* embryos reveals translational control of the segmentation gene hunchback. *Chromosoma*. 98:81–85.

Tetzlaff, M.T., H. Jackle, and M.J. Pankratz. 1996. Lack of *Drosophila* cytoskeletal tropomyosin affects head morphogenesis and the accumulation of oskar mRNA required for germ cell formation. *EMBO (Eur. Mol. Biol. Organ.) J*. 15:1247–1254.

Theurkauf, W.E., and T.I. Hazelrigg. 1998. In vivo analyses of cytoplasmic transport and cytoskeletal organization during *Drosophila* oogenesis: characterization of a multi-step anterior localization pathway. *Development*. 125: 3655–3666.

Thieringer, H.A., K. Singh, H. Trivedi, and M. Inouye. 1997. Identification and developmental characterization of a novel Y-box protein from *Drosophila melanogaster*. *Nucleic Acids Res*. 25:4764–4770.

Wang, S., and T. Hazelrigg. 1994. Implications for bcd mRNA localization from spatial distribution of exu protein in *Drosophila* oogenesis. *Nature*. 369:400–403.

Wilhelm, J.E., and R.D. Vale. 1993. RNA on the move: the mRNA localization pathway. *J. Cell Biol*. 123:269–274.

Wilsch-Brauninger, M., H. Schwarz, and C. Nusslein-Volhard. 1997. A sponge-like structure involved in the association and transport of maternal products during *Drosophila* oogenesis. *J. Cell Biol*. 139:817–829.

Yurkova, M.S., and M.T. Murray. 1997. A translation regulatory particle containing the *Xenopus* oocyte Y box protein mRNP3+4. *J. Biol. Chem*. 272: 10870–10876.